Advanced Micro-Grids

Raveesha.S.H[1], Ashoka.H.N[2]

[1]Asst.Professor, SBIT Tiptur,
[2]Associate Professor, UBDTCE Davanagere

Abstract: *In modern society every sector needs continuous power on demand. To achieve this voltage, current and frequency, these parameters of the power system should be at rated values. Because of remote generation, transmission and distribution, we are failing to receive the reliable power. To overcome this problem, the Distribution energy sources (DES) become more suitable solution. This generated power from DES is supplied to local loads and this can be connected to the main grid through the Micro-Grid (MG). Micro-grids will operate in two modes, A Grid-connected mode and in an Islanded mode. During islanding mode, one Distributed Generation (DG) unit should share output generation power with other unit in exact accordance with the load. Need to control Real and Reactive power effectively for the load to operate without disturbance. Hence in the present work, Voltage Source Inverter (VSI) and Proportional Integral Derivative(PID) controller in power conversion process to get required real and reactive power for the normal operation of micro-grid. The proposed method has been applied to a designed test Simulink model for different types of Grid connected and Isolated modes. The simulation results obtained show that, this method can improves the reliability and smooth operation of the micro-grid system.*

Index Terms: *Distributed generation, PID control, micro-grids,*

I. Introduction

Distributed generation also called local generation [1]-[4]. Where the power is generated there itself distributed the power, generates power from many small energy sources, Solar power , Wind power, Bio-gas, Fuel cell etc. Distributed generation (DG) identified as one of the mechanism for ensuring supply of power in rural areas, remote areas, and hilly areas by way of setting up small generating units based on a variety of local fuel along with localized distribution. Usually conventional plants are for away from the populated area, so transmit the power from generation plant to distribution power network, cost of transmission will be more and protection for this system is need more compare to the Distributed generation.

Distributed generation used to supply the power continuous and quality of power supply, Distribution generation it is more necessary in the power system. Distributed generation for flexible operation Micro grid, mainly classified into three type, Distributed generation, Micro-Grid and control system [4].

A micro grid is design to seamlessly separate from the grid when problems in the utility grid arise, reconnecting again once these problems are resolved [15]. Normally in grid connected mode, the micro sources act as constant power sources, which are controlled to inject the demanded power into the network. In autonomous mode, micro sources are controlled to supply all the power needed by the local loads while maintaining the voltage and frequency within the acceptable operating limits.

II. Control Required

Reactive power is essential to maintain and control voltage in AC electrical systems. The ability to meet the demand for rapid changes in reactive power prevents instability, voltage sags, even voltage collapse. Newer technology, such as the DSTATCOM Distribute Static Compensator offers a better solution to voltage stability problems. in that DSTATCOM includes Voltage source Inverter (VSI), Current Converter(C-C). PID [12]. The DSTATCOM generates a variable voltage V_d, that is very nearly in phase with the source voltage Vs. The inductance in this simplified circuit, L, consists of the inductance of the coupling transformer and filter. The voltage across the inductance, V_L, equals V_s-V_d. If Vs > V_d, V_L is in phase with V_s and current I_L lags V_s by 90°, DSTATCOM acting as a generator produces leading reactive current. If V_s < V_d, V_L is anti phase with V_s and current I_L leads V_s by 90°, DSTATCOM produces lagging reactive current[5].

DSTATCOM used to control the inner loop and outer loop. DSTATCOM is an Independent control of these quantities can be achieved with the using Clark transformation

$P = v_q . i_q + v_d i_d$ ………………………… (1.1)

$Q = v_q . i_d - v_d i_q$ …………………………... (1.2)

Where P =Active power,
Q =Reactive power
v_d=Real voltage
v_q=Imaginary voltage,
i_d=Real current,
i_q=Imaginary current

Normally, for rotating machines the d-axis of the d_q-reference system is chosen at the rotor of the machine. This leads to $v_d = VSTATCOM$ and $v = 0$ and hence for the active and reactive power using equation (1.1 and 1.2)

$P = v_d \cdot i_d$…………………..…..………….. (1.3)
$Q = -v_d \cdot i_q$…………………..…………. (1.4)

The transformation into the rotating d-reference frame leads to the possibility to control the two current components i_d and i_q independently and hence control the active and reactive power independently.

Therefore static errors in the control system can be removed   by applying PID controllers. The STATCOM controls the voltage by injecting or absorbing reactive power and q-axis current component of the current has to be controlled.. The output of the controllers is brought to a limiter block which limits the output of the controllers and provides the reference values for the inner controller loop. The output signal i_{dref} is limited
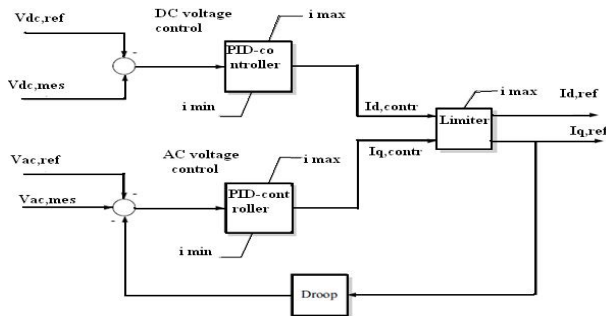

Figure.1.10. STATCOM outer control loop

$$i_{d,ref} = \begin{cases} -i_{max} & if \quad i_{d,contr} < -i_{max} \\ i_{max} & if \quad i_{d,contr} > i_{max} \\ i_{d,contr} & if -i_{max} < i_{d,contr} < i_{max} \end{cases} ..(1.5)$$

For the limitation of i_{qref} as follows
$i_{q,ref}$

$$= \begin{cases} -i_{max} + |i_{d,ref}| & if \quad i_{q,contr} < -i_{max} + |i_{d,ref}| \\ i_{max} - |i_{d,ref}| & if \quad i_{q,contr} > i_{max} - |i_{d,ref}| \\ i_{q,contr} & if -i_{max} + |i_{d,ref}| < i_{q,contr} < i_{max} - |i_{d,ref}| \end{cases}$$
…………………………….(1.6)

The block scheme of the inner controller loop is given in figure 1.11. The inner controllers consist of two regular PID-controllers which are much faster than the outer loop controllers. The output of the inner controllers is the modulation index M_d and M_q which actually control the converter
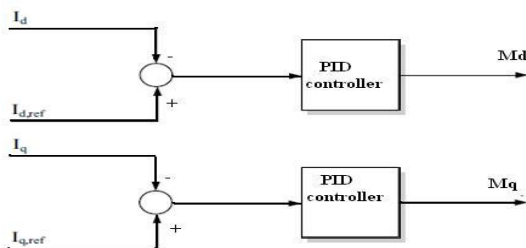

Figure 1.11. STATCOM inner loop control

III. Control system Design

3.1. Physical Model Design
3.1.1 System Configuration
Fig.3.1. shows the micro-grid system under study, which is adapted from the IEEE 1559 standard for low voltage applications [17]. The adopted study system represents a general low voltage distribution system, where different types of loads and different numbers of DG units can be considered to be connected to the main feeder. The DG units can be employed to work either parallel to the utility grid, or in isolated mode to serve sensitive loads connected to the main feeder when the main breaker (BR) is open. Without loss of generality, the performance of the micro-grid system is studied under the presence of two DG units, supplying general types of loads. The load on the second feeder is an inductive load where a 2.5-KVAr power factor correction capacitor bank is also considered to be connected to the main feeder. The adopted load model is in line with the IEEE 1547 test load used in DG applications. The nonlinear load is a three-phase diode rectifier with an R-L load at the dc-side. The addition of the diode rectifier helps in assessing the effectiveness of the proposed controller in rejecting voltage harmonics associated with nonlinear loading, and rejecting load-DG-unit-grid interactions at harmonic frequencies. The schematic diagram of a single DG unit as the building block of the sample micro-grid system is also shown in Fig.3.1. When the DG unit is connected to the grid, the voltage and frequency at the point of common coupling are dominantly dictated by the grid. However, in case of weak grids, the voltage is prone to voltage sags and disturbances. In this case, the DG unit can be controlled to support the grid voltage. Therefore, both PQ and PV operational modes can be adopted in the grid- connected mode. Subsequent to an islanding event, DG

$$Z_{\alpha\beta} = Z_{\alpha} + jZ_{\beta} \dots\dots\dots\dots\dots\dots\dots (3.2)$$

Using (3.2), the state space model of the system in the $\alpha\beta$ frame is as follows

$$\frac{d_{il,\alpha\beta}}{dt} = -\frac{V_{o.\alpha\beta}}{L} + \frac{V_{inv,\alpha\beta}}{L}$$
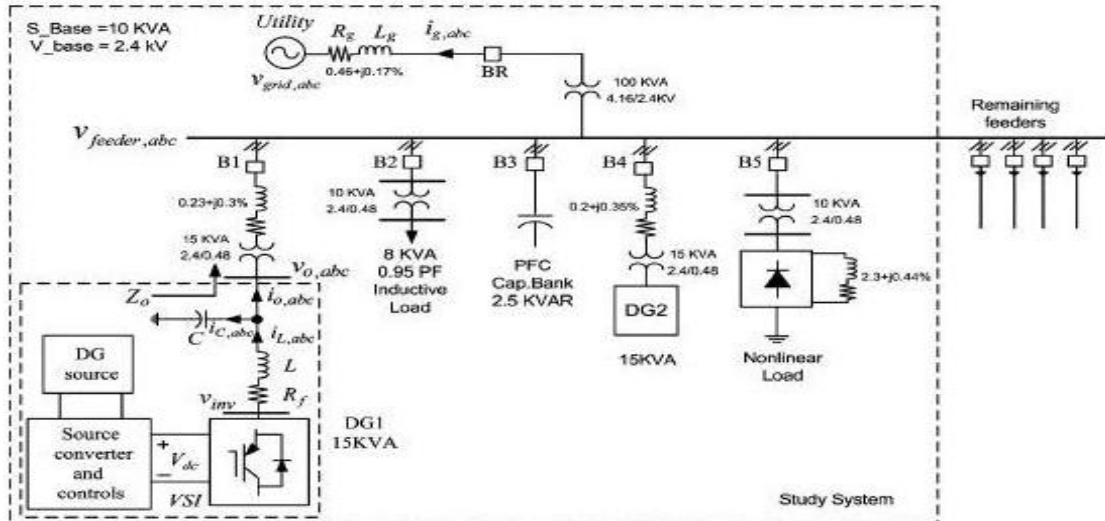

Fig.3.1. IEEE 1559 Single line diagram of the micro-grid study system

units can form an autonomous micro-grid system to enhance the reliability of sensitive loads[13]-[15]. In both grid connected and isolated modes, the state space presentation of the DG interface dynamics can
Be given in the natural frame

.

$$V_{inv,abc} = L\left(\frac{d_{iL,abc}}{dt}\right) + V_{o,abc}$$

$$i_{L,abc} = i_{o,abc} + i_{c,abc} = i_{o,abc} + C\left(\frac{d_{vo,abc}}{dt}\right)..(3.1)$$

where L and C are the filter inductance and capacitance, $V_{inv,abc}$ is the inverter output voltage, $i_{L,abc}$ is the inverter output current, $V_{o,abc}$ is the voltage at the point of common coupling, and $i_{L,abc}$ is the network-side current. Note that $V_{inv,abc}$, $i_{L,abc}$ $V_{o,abc}$ and $i_{o,abc}$ are 3×1 vectors representing phase quantities corresponding to each phase, and the filter-inductor resistance is ignored. In order to decrease the number of differential equations and simplify system presentation, (3.1) can be rewritten in a stationary $\alpha\beta$ reference frame system by applying the following a b c to $\alpha\beta$ transformation.

$$Z_{\alpha\beta} = Za_{e^{j0}} + Zb_{e^{j(-\frac{2\pi}{3})}} + Zc_{e^{j(\frac{2\pi}{3})}}$$

$$\frac{d_{vo,\alpha\beta}}{dt} = \frac{i_{L,\alpha\beta}}{L} - \frac{i_{o,\alpha\beta}}{L} \dots\dots\dots\dots\dots\dots\dots (3.3)$$

Fig.3.2 the block diagram representation of the differential equations derived in (3.3) where models the disturbance caused by connecting the system to the utility grid. The block diagram suggests that the output current (i.e.i_o) can be regarded as an external disturbance caused by unknown load or grid behavior either in islanded or grid connected mode. Along with these disturbances, control mode switching in conventional DG controllers generates internal disturbances within the control structure.

3.1.2. Control Structure

As indicated in Fig. 3.2, external disturbances will be imposed on the DG interface during mode transition and network/load disturbances. On the other hand, internal disturbances will be generated due to control function switching between different modes in the conventional hierarchical control structure. To overcome these issues and to achieve a flexible and robust operation of DG units under the smart grid environment while maintaining the hierarchical control structure, the proposed control scheme, shown in Fig.3.2, utilizes a fixed hierarchical power–voltage–current control structure in both grid-connected and isolated modes[4]-[11].This will minimize the undesired voltage transients generated by switching from a current-controlled interface to a voltage-controlled interface in conventional control techniques. Further, the proposed power controller works under grid-connected and isolated micro-grid modes. This feature provides a flexible interface for the DG unit to be used in different operational modes with minimal switching. Due to the proposed design strategy, both external and internal disturbances can be eliminated or remarkably attenuated within the DG interface. Moreover, the fixed control structure increases the robustness of the control structure to islanding detection delays. The voltage control is designed by considering an augmented model that includes the LC-filter active damping and inner current control loop dynamics to ensure robustness and coordinated control design. Theoretical analysis and design procedure of the proposed control scheme are described in the following sections.
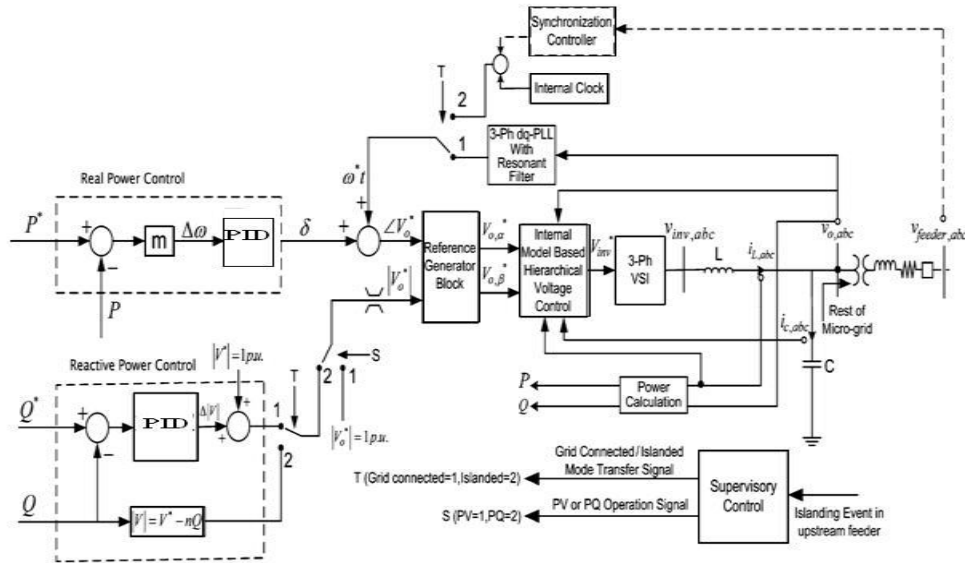

Fig.3.2. Control scheme

In resonance damping applying an LC filter at the output stage introduces a resonance peak to the frequency response of the system, which can limit the achievable bandwidth of the current controller in a multi loop hierarchical control approach. Besides, as the filter and grid parameters change, the corresponding resonance frequency also shifts, resulting in potential harmonic excitations at low-order harmonics affecting system stability. Therefore converter resonance damping is essential to maintain stability and facilitate high bandwidth current control design. Active damping
resonance damping can be a viable option, particularly in DG applications and effective technique to actively damp filter resonance is to introduce a damping voltage that is proportional to the capacitor current. The dynamic equations corresponding to the actively damped system can be given as follows

$$L\frac{di_{L\alpha\beta}}{dt} = (v_{inv,\alpha\beta} - v_{d)} - v_{o,\alpha\beta} \ldots\ldots\ldots\ldots (3.4)$$

$$v_{d=} R_d \ i_c \quad \ldots\ldots\ldots\ldots\ldots\ldots\ldots\ldots (3.5)$$

Where V_d represents the current-dependent voltage source injected in series with the original inverter output voltage and R_d is the virtual damping coefficient. With the active damping voltage modeled as a current-controlled voltage source, the open loop transfer function of the system is driven

$$G_{(s)} = \frac{V_{o,\alpha\beta}}{V_{inv,\alpha\beta}} = \frac{1}{LC_{s}2 + R_d C_s + 1} \ldots\ldots\ldots\ldots (3.6)$$

on the open loop system frequency characteristics. The resonance peak can be completely damped, and accordingly high control band width R_d can be achieved can provide the desired damping performance. A newly designed augmented internal model control (IMC) structure is proposed to provide internal model dynamics for harmonic, unbalanced, and random voltage disturbances.

Under exact model matching (i.e., $G_m(s) = G(s)$) and the absence of system disturbances, the feedback signal, which is influenced by the disturbance or any model uncertainties, would be zero. In this case, the IMC structure[16], shown in Fig.3.3, regarded as an open loop system where the feed-forward compensator should be designed to ensure close tracking performance .On the other hand, disturbance rejection achieved via the feedback compensator design. Since the tracking and disturbance rejection performances can be designed independently, the IMC control scheme .The sensitivity function(S) and the complementary sensitivity function (T), which represents tracking and
Disturbance rejection capabilities of the system, respectively, driven as follows

$$S_{(s)} = \frac{y(s)}{d(s)} r = 0$$

$$S_{(s)} = \frac{1}{1 + G_{m(s)} Q_{d(s)}} \ldots\ldots\ldots\ldots\ldots\ldots\ldots (3.7)$$

$$T_{(s)} = \frac{Y(s)}{r_{(S)}} d = 0$$

$$T_{(S)} = \frac{G_{(S)} Q_{r(S)} (1 + G_{m(S)} Q_{d(S)})}{1 + G_{m(S)} Q_{d(S)}} \ldots\ldots\ldots\ldots\ldots (3.8)$$

The design goal is then to propose   and   such that   and within a reasonably large range of frequencies of interest. This assures both disturbance rejection and tracking ability of the system. Assuming and then the model following error (e) is zero and the control scheme is reduced to an open loop one with T((s))=Q(r(s))G((s)) Performance stability constraints require an improper transfer function and cannot be realized practically. Therefore, a low pass filter is used to yield a proper feed-forward compensator

$$Q_{r(S)} = \frac{1}{(\tau s + 1)^n} \cdot G_{m(S)}^{-1} \ldots\ldots\ldots\ldots (3.9)$$

Where τ corresponds to the bandwidth of the filter, and n is an integer selected in such a way that $Q_{r(S)}$ is a proper function. The disturbance rejection is achieved via $Q_{d(S)}$ which produces a compensating
input to cancel out disturbances. To overcome the computational burden associated with frame a transformation, the proposed controller is performed in $\alpha\beta$ - frame. Proportional Integral derivative resonant controller used removes the harmonic.

The augmented model simplified as shown in Fig.3.5, where $G_{(S)}$ models the transfer function between V_{inv} and v in the presence of the active damping loop. The output/input transfer function is given by

$$\frac{V_o}{i_L} = \frac{K_C L}{L^2 C_S^2 + (K_C L_C + R_d LC)s + (L + K_C R_d C)} \quad \ldots\ldots\ldots (3.10)$$

IMC-based multi loop voltage control structure. Considering the output/input relation calculated in (3.10) and the design approach introduced in (3.9), Q$_r$(s) given by (3.11), where "m" denotes nominal model parameters.

$$Q_{r(S)} = \frac{L_m^2 C_{ms}^2 + (K_C L_m C_m + R_d L_m C_m)s + (L_m + R_d K_C C_m)}{K_C L_m (\tau s + 1)^2} \quad ..(3.11)$$

It can be noted that the feed-forward compensator is both stable and proper. The time constant τ dictates the tracking bandwidth of the system. It can be also noted that mismatch in system parameters can be considered as disturbances and it will be attenuated by the feedback compensators. The sensitivity transfer function of the proposed system, which represents the frequency response of the $\frac{V_o}{I_o}$ transfer function, can be also obtained from

$$\frac{V_o}{I_o} = \frac{L_s}{K_C Q_{d(s)} + LC_S^2 + (R_d C + K_C C)s + 1} \quad \ldots\ldots\ldots\ldots\ldots (3.12)$$
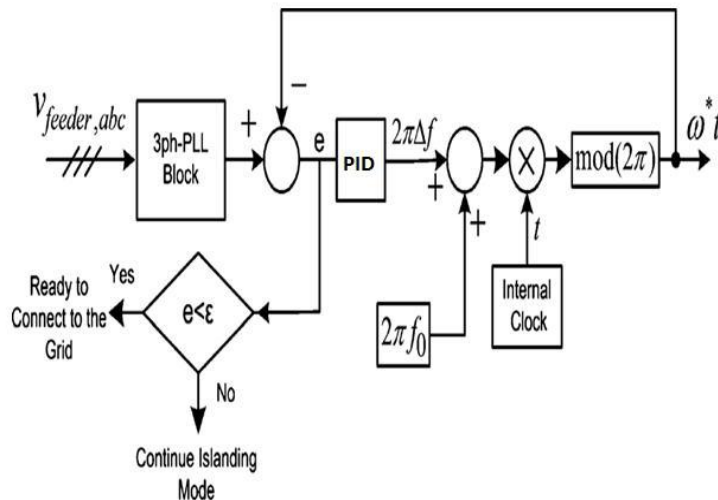

Fig.3.8. Synchronization controller

Power flow control adopted hierarchical design approach provides flexible operation of the DG unit in grid-connected mode [17]-[20]. To minimize the control switching actions between grid-connected and isolated modes, a single active power control structure is used in both modes. The proposed active power controller, shown in Fig.3.2, consists of a slow integrator, which generates frequency deviations $\Delta\omega$ according to the power-frequency characteristics presented in (3.13)

$$\Delta\omega = m(P^* - P) \ldots\ldots\ldots\ldots\ldots\ldots\ldots (3.13)$$

The above equation (3.13) is very similar to the frequency-power droop equation in autonomous micro-grid system by adopting an appropriate slope coefficient (i.e., m) based on a reasonably small frequency deviation range, in the grid-connected mode, the phase angle of the grid $\omega^* t$ is generated via a dq three-phase phase-locked loop[5].PLL during islanded operation, the processor internal clock is used to generate the a signal ω^* while is assumed to be100 .Considering the voltage and reactive power controller, the voltage amplitude can be either set to 1.0 p. u. for PV-bus operation . In the grid-connected mode, a
Proportional integral derivative (PID) controller is adopted to provide the magnitude of the output voltage |V |.Therefore, the voltage control signal can be generated in islanded operation; however, a voltage droop function is adopted to share the reactive power among different DG units. Accordingly, the voltage magnitude is generated according to

$$|V_o| = V^* - nQ\ldots\ldots\ldots\ldots\ldots\ldots\ldots\ (3.14)$$

Where n is the reactive power droop gain PLL configuration and Synchronization Fig. 3.8 can be realized by applying small frequency deviations in the voltage command to decrease the phase mismatching between the two voltages.

IV. Results And Discussion

To evaluate the performance of the proposed control scheme, the study system depicted in Fig.3.1 is implemented for time domain simulation under the Mat lab/Simulink. The proposed flexible control structure, shown in Fig. 3.2. Different modes are tested results are presented as follows

4.1. Grid-Connected Mode

Fig.4.1 and 4.2 shows the control performance under PQ-bus operation mode for one of the DG units. The inductive load and the capacitor bank are activated in this scenario. The reactive power command is set to zero, whereas the active power command experiences a step change from 6 to 10 kW at t=1s. Fig.4.1 (1) and (2) shows the active and reactive powers generated by the unit. Close active power tracking performance. On the other hand, the coupling between active and reactive power dynamics is minimal. Fig.4.2 (1) depicts how the output voltage amplitude changes to maintain the unity power factor condition while increasing the active power injection .Voltage fluctuation in this mode is the natural result of the absence of voltage control at the point of common coupling. The instantaneous phase-a output voltage is shown in Fig.4.2 (2).In addition to active power regulation, the DG unit can contribute to the voltage reliability at the point of common coupling by allowing bus voltage control i.e., PV mode. This mode can be activated once voltage sags are detected. Under these conditions, the voltage control mode is activated to inject reactive power during the sag period to provide fault-ride-through performance. Accordingly, the economic operation of the DG unit will not be compromised. On the other hand, in long radial feeders and weak grids, existing DG units can be used for continuous voltage support.

Fig.4.3 &4.4 shows the effectiveness of the proposed control strategy in terms of providing the DG unit with the fault-ride-through capability. The grid voltage encounters a 10% sag from t=1s to t=1.25sdue to an upstream fault in the main feeder. The R-L-C load is Fig.4.3 &4.4 shows the effectiveness of the proposed control strategy in terms of providing the DG unit with
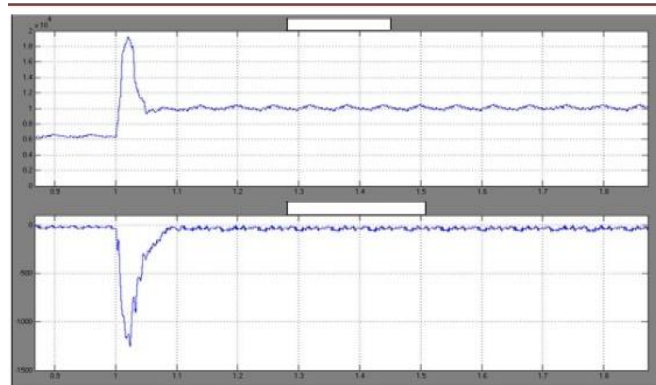

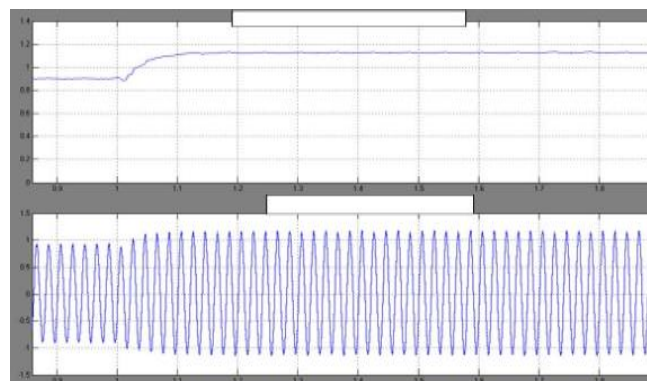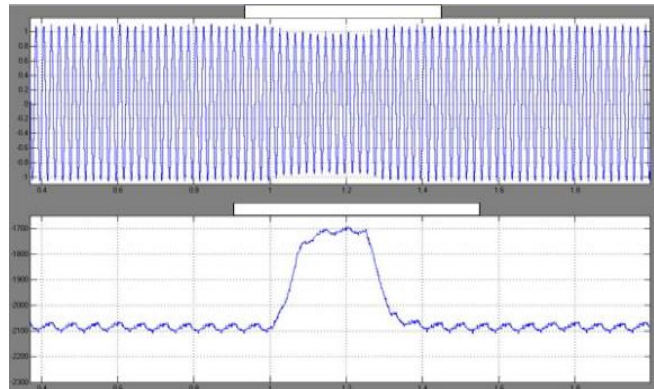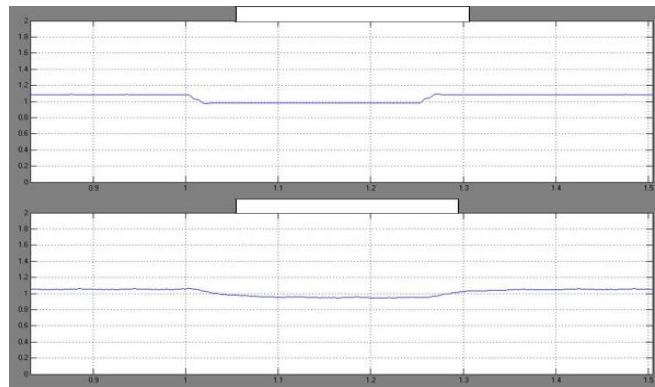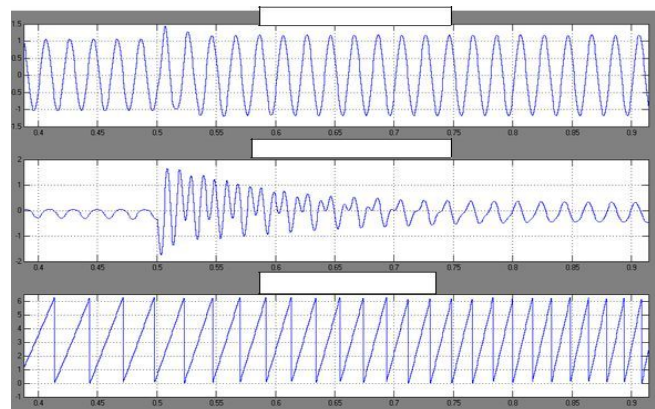**Fig. 4.1**. (1) Converter active power. (2) Converter reactive power

Fig.4.2. (1) Output voltage magnitude. (2) Instantaneous phase-a output voltage

Fig. 4.3(1) Instantaneous output voltage. (2) Converter reactive power

Fig.4.4 (1)Feeder voltage in p.u. (2) DG output voltage

Fig.4.5. (1) Phase- a output voltage. (2) Phase-a load current (3) PLL output,

the fault-ride-through capability. The grid voltage encounters a 10% sag from t=1s to t=1.25s due to an upstream fault in the main feeder. The R-L-C load is assumed to be the locally connected load. Fig.4.3 (1) shows the phase-voltage during the voltage disturbance.Fig.4.3 (2) shows the reactive power injected by the unit during the fault period. Fig.4.4 (1) shows the magnitude of the output voltage of the main feeder. Fig.4.4 (2) shows the magnitude of the output voltage of the DG unit. Provided that there is enough reactive power rating, larger voltage sags can be mitigated by the DG interface.

To test the disturbance rejection against loading transient's band harmonic loading, the nonlinear load is switched ON at t=0.5s. The controller response to the addition of the nonlinear load is shown in Fig.4.5. Fig.4.5 (1) shows the output voltage waveform of phase-a, whereas Fig.4.5 (2) shows the load current. The proposed controller acts fast enough to reject the sudden loading disturbance yielding close voltage regulation at the local ac bus voltage. On the other hand, the harmonic disturbance rejection ability of the proposed controller is obvious. In spite of the heavily distorted load current, the total harmonic distortion (THD) of the phase-a voltage is 0.67% and 0.81% before and after adding the nonlinear load, respectively. The PLL output in the presence of harmonics is also shown in Fig.4.5 (3). Note that the PLL output is robust even after adding the rectifier load to the system. This is because of the resonant filter which provides robust phase tracking in the

presence of harmonics. These results confirm the high disturbance rejection performance of the proposed controller.

4.2 Isolated Mode

The transitional performance of the study system under the proposed control scheme from grid connected to islanded mode is evaluated by emulating an islanding event via opening the breaker switch (BR) at the upstream feeder in Fig.3.1. Initially, the micro-grid system is connected to the grid and both DG units are working in the PV-bus mode. The study system is islanded at t=0.8s by opening the breaker BR. feeder breaker goes open and this event is signaled to the supervisory control unit shown in Fig.3.2. The detection delay is assumed to be 20 ms, therefore, the islanding event is detected at t=0.82s.

Fig.4.6 the dynamic response of the system before and after the islanding event. DG units utilize the same control structure, which is applied for both grid connected and islanded modes. Reactive power sharing is adopted in the isolated mode. The load voltage waveform and magnitude are shown inFig.4.6 (1) and (2), respectively. In Fig.4.6 (1), the voltage response associated with the conventional method (i.e., from current-controlled to switching voltage-controlled interface) is also shown. As it can be seen, without applying the proposed method, the system is experiencing much higher over voltages due to the internal disturbance generated by switching from
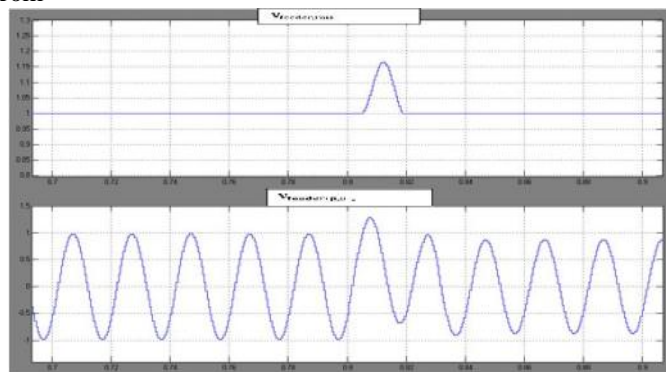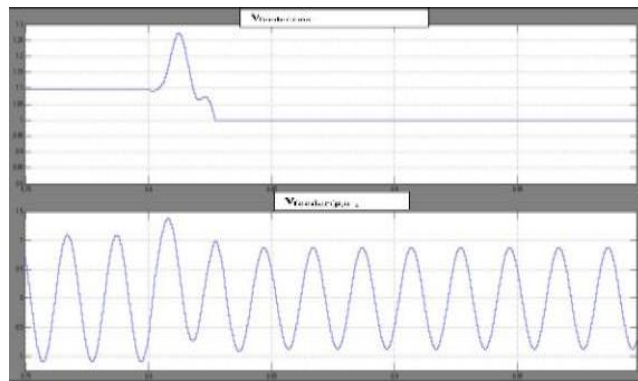

Fig.4.6. (1) RMS feeder voltage with proposed controller. (2) Instantaneous phase- a grid voltage with proposed controller
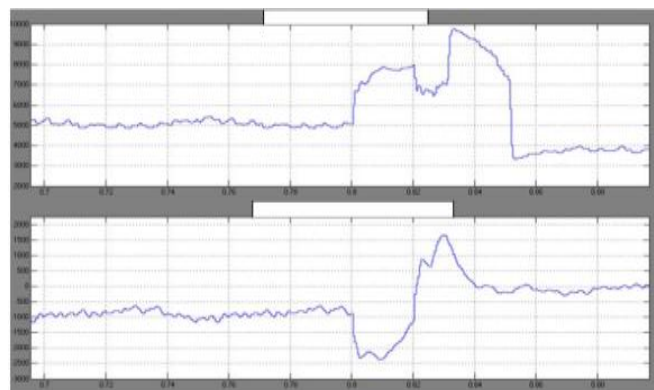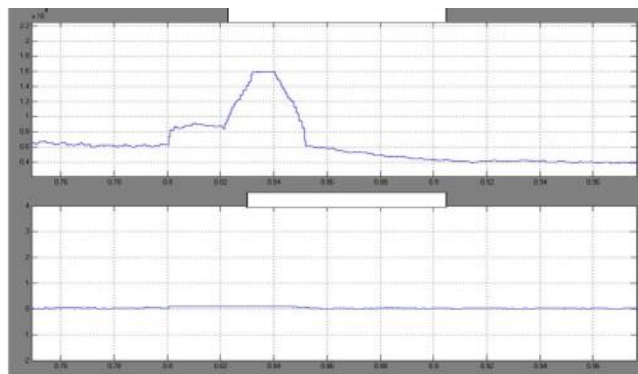

Fig.4.7. (1) Active converter powers of DG1 unit, (2) Reactive converter powers of each DG1 unit
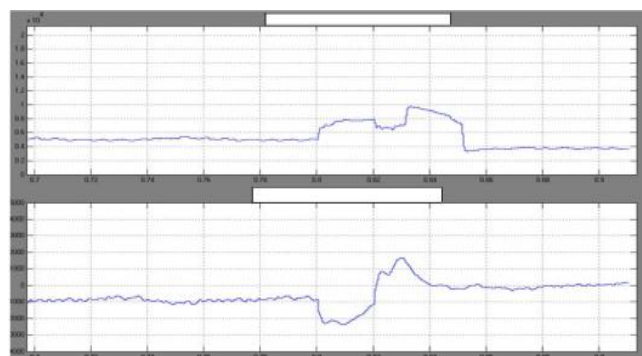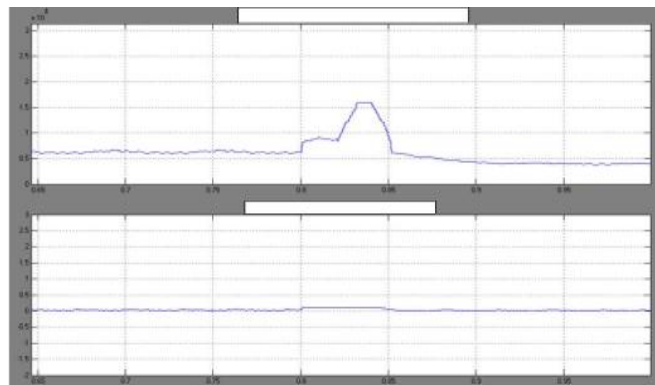

Fig. 4.8. (1) Active converter powers of DG2 unit, (2) Reactive converter powers of each DG2 unit
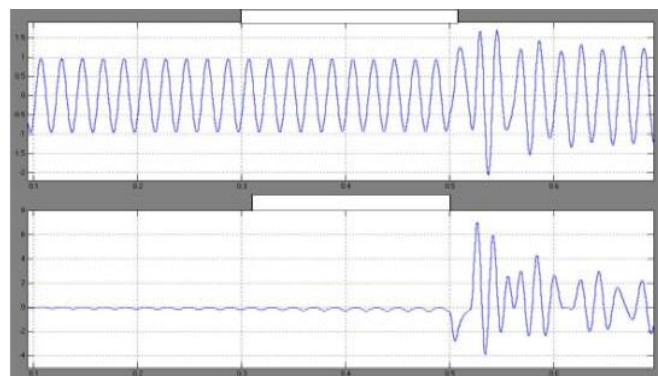
Fig.4.9. (1) RMS feeder voltage with proposed controller.. (2) Instantaneous phase- a grid voltage with proposed controller
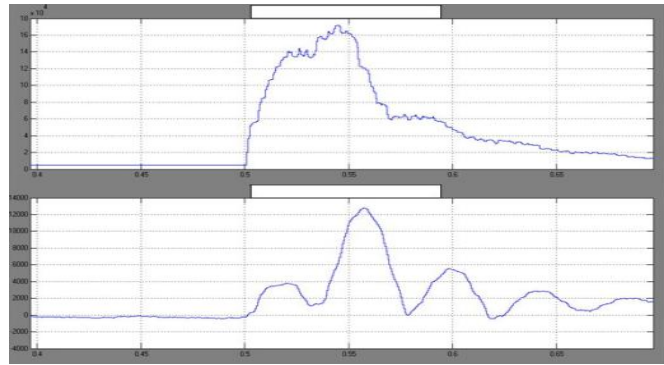

Fig.4.10.. (1) Active converter powers DG1 unit,(2) Reactive converter powers of each DG1 unit
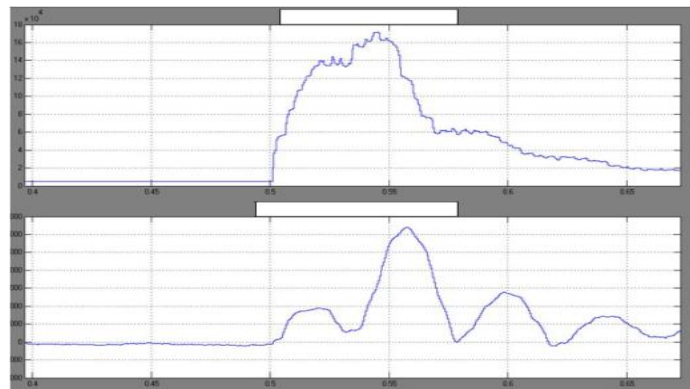

Fig.4.11. (1) Active converter powers of DG2 unit,(2) Reactive converter powers of each DG2 unit
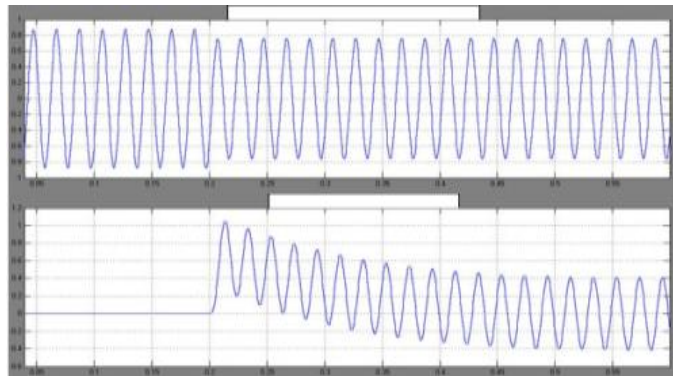

Fig.4.12. (1)Instantaneous phase-a output voltage. (2) Phase-a load current
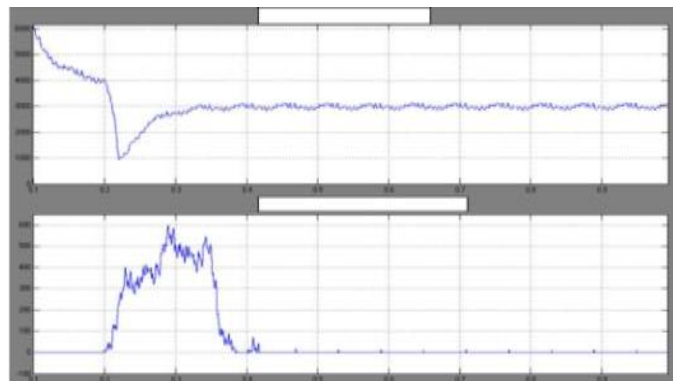
Fig.4.13. (1) Active converter powers for DG1. (2) Reactive converter powers for DG1
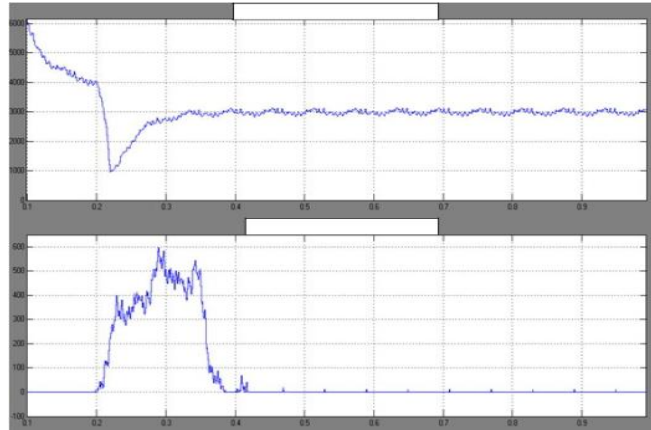

Fig.4.14. (1) Active converter powers for DG2. (2) Reactive converter powers for DG2

Fig.4.15. (1) Instantaneous phase-a output voltage. (2) Instantaneous phase-a grid current

Fig.4.16 (1) Active converter powers for each DG1 unit.(2)Reactive converter powers for each DG1 unit

Fig.4.17. (1) Active converter powers for each DG2 unit, (2) Reactive converter powers for each DG2 unit.

Current-controlled interface to a voltage-controlled subsequent to an islanding event. The dynamics responses of the active and reactive power components for each DG unit are shown in Fig. 4.7 and 4.8, where the initial active power generated by each DG1 and DG2, dictated by the power controller in the grid connected mode. However, subsequent to the islanding event, the generated active power is decreased in order to meet the load consumption. For further performance, the micro-grid system is connected to the grid and both DG units are working in the PQ-bus mode with unity power factor. The utility supply is lost at t=0.8 s. The islanding is detected after 20 ms by the supervisory control unit at t=0.82s. Fig.4.6, 4.7 & 4.8 depicts the dynamic response of the system prior and after the islanding event. The magnitude and load voltage waveform are shown in 4.9(1) and 4.9(2) respectively. Close voltage control characteristics are yielded subsequent to the islanding event. Once again the system response in the absence of the proposed scheme is shown in Fig.4.9 (2), where the higher transient over-voltage is obvious. The active and reactive power responses for DG units are shown in Fig.4.10 and 4.11, where the initial active power generated by each DG is 6.0 kW at unity power factor. Subsequent to the islanding event, the generated active power decreases in order to meet the load demand

Fig.4.12, 4.13 and 4.14 shows the load voltage and current responses of the islanded system when the nonlinear load is added at t=0.5s. Fig.4.12 (1) shows the load voltage, whereas Fig. 4.12(2) shows the load current. It can be seen that the controller is well capable of maintaining the output voltage quality despite the highly distorted current going through the load. The THD of the load voltage is 2.7%. Fig. 4.13 shows the active and reactive power profiles of both DG1 units.4.14 Shows the active and reactive power profiles of DG2 units accurate power sharing performance is yielded even in the presence of harmonic loading, which demands reactive power injection by both DG units.

Fig.4.15, 4.16 and 4.17 shows the grid current, the load voltage, and power responses during a supply restoration scenario at t=0.2s. Once the utility supply is restored, both DG units operate as a PQ bus with unity power factor and with a power command of 3.0 kW for each unit. In spite of grid-current transients, the load voltage is closely controlled to facilitate seamless restoration. Similar to the micro-grid formation event, the proposed control scheme yield seamless connection performance under the supply restoration event by rejecting the generated disturbances internally and externally within the control structure

PID,VSI used control the different mode of operation, maintaining constant real and reactive power during islanding and grid connected mode condition, compared to the PI controller PID controller utilizes a fixed power-voltage-current cascade control structure with robust internal model voltage controller to maximize the disturbance rejection performance within the DG interface and to minimize control function switching and also facilitates flexible DG operation in the grid-connected mode and autonomous micro grid.

V. CONCLUSION

The Simulink model has been design for the proposed test system and analyzed the simulation results for isolated mode and grid connected mode of the proposed test system. Be the simulation results we can conclude that, the following parameters can be controlled efficiently and in better way;

- It provides current limit capability for the Converter during grid faults.
- DGs shared the proper amount of power via proposed method.
- A start-up PLL based turn ON techniques to eliminate the circulating current completely during the turn ON the new incoming unit.
- Fast voltage regulation and effective mitigation dynamic, unbalanced voltage and harmonic voltage

disturbances.
- The proposed voltage and power sharing controller provide high disturbance rejection performance against voltage disturbances and power angle swing.
- It provides smooth transition capability between grid-connected and autonomous (islanded) modes.

The proposed control scheme enhances the flexibility of Micro-grid operation under the dynamic nature of future smart distribution system.

REFERENCES

[1.]   E.M.Lightener and S. E. Widergren, "An orderly transition to a transformed electricity systems," IEEE Trans. Smart Grid, vol. 1, no. 1, pp.3–10, Jun. 2010

[2.]   K.Molehill and R. Kumar, "A reliability perspective of smart grid,"IEEE Trans. Smart Grid, vol. 1, no. 1, pp. 57–64, Jun. 2010.

[3.]   G.T.Heydt, "The next generation of power distribution systems,"IEEE Trans. Smart Grid, vol. 1, no. 3, pp. 225–235, Nov. 2010

[4.]   A.Timbus, M. Liserre, R. Teodorescu, P. Rodriquez, and F. Blaabjerg,"Evaluation of current controllers for distributed power generation systems,"IEEE Trans. Power Electron., vol. 24, no. 3, pp. 654–664, Mar.2009

[5.]   J.M.Guerrero, J. C.Vasquez, J.Matas, K.Vicuna, and M. Castilla, "Hierarchical control of droop-controlled ac and dc micro grids A general approach towards standardization," IEEE Trans. Ind. Electron., to be published.

[6.]   M.Liserre, R. Teodorescu, and F. Blaabjerg, "Multiple harmonics control for three-phase grid converter systems with the use of PI-RES current controller in a rotating frame," IEEE Trans. Power Electron., vol.21, no. 3, pp. 836–841, May 2006.

[7.]   Y.A.-R.I.Mohamed, "Mitigation of dynamic, unbalanced and harmonic voltage disturbances using grid-connected inverters with LCL filter," IEEE Trans. Ind. Electron., vol. 58, no. 9, pp. 3914–3924, Sep.2011.

[8.]   S.Ahn,"Power-sharing method of multiple distributed generators considering modes and configurations of a micro grid," IEEE Trans. Power Del., vol. 25, no. 3, pp. 2007–2016, Jul. 2010.

[9.]   Twinning and D.G. Holmes, "Grid current regulation of a three phase voltage source inverter with an LCL input filter," IEEE Trans. Power Electron., vol. 18, no. 3, pp. 888– 895, May 2003

[10.]   D.De and V. Ramanarayanan, "Decentralized parallel operation of inverters sharing unbalanced and nonlinear loads," IEEE Trans. Power Electron., vol. 25, no. 12, pp. 3015–3022, Dec. 2010.

[11.]   H.Kim,T.Yu, and S. Choi, "Indirect current control algorithm for utility interactive inverters in distributed generation systems," IEEE Trans. Power Electron., vol. 23, no. 3, pp.1342–1347, May 2008

[12.]   Y.A.-R.I. Mohamed, "Mitigation of grid-converter resonance, grid-induced distortion and parametric instabilities in converter-based distributed generation," IEEE Trans. Power Electron., vol. 26, no. 3, pp.983–996, Mar. 2011.

[13.]   Z.Yao,L.Xiao, and Y.Yan, "Seamless transfer of single-phase grid interactive inverters between grid connected and stand-alone modes,"IEEE Trans. Power Electron., vol. 25, no. 6, pp. 1597–1603, Jun. 2010.

[14.]   F.Gao and R.Iravani, "A control strategy for a distributed generation unit in grid-connected and autonomous modes of operation," IEEE Trans. Power Del., vol. 23, no. 2,pp.850–859, Apr. 2008.

[15.]   Y.A.-R.I.Mohamed and A. Radwan, "Hierarchical control system for robust micro-grid operation and seamless mode-transfer in active distribution systems," IEEE Trans. Smart Grid, vol. 2, no. 2, pp. 352–362, Jun. 2011.

[16.]   M.Morari and E. Zafirious, Robust Process Control. Englewood Cliffs, NJ: Prentice Hall, 1989, ch. 2–3.

[17.]   F.Blaabjerg, R.Teodorescu, M.Liserre, and A.V.Timbus, "Overview of control and grid synchronization for distributed power generation systems," IEEE Trans. Ind. Electron., vol. 53, no. 5, pp. 1398–1409,Oct. 2006.

[18.]   Draft Guide for Design, Operation, and Integration of Distributed Resource Island Systems With Electric Power Systems, IEEE P1547.4.

[19.]   W. Xu,G. Zhang, C.Li,W.Wang, G.Wang, and J. Kliber, "A power line signaling based technique for anti-islanding protection of distributed generators–Part I: Scheme and analysis," in Proc. 2007 IEEE Power Engineering Society General Meeting, Jun. 24–28, 2007, p. 1.

[20.]   M.A.Redfern, O. U.Usta, and G. Fielding, "Protection against loss of utility grid supply for a dispersed storage and generation unit," IEEE Trans Power Del., vol. 8, no. 3, pp. 948–954, Jul. 1993